

SPECTRAL ANALYSIS OF A TURBULENT WARM PLANE AIR JET (Using hot-wire anemometry)

S. Amiri^{1,2}, M. Sandberg² and B. Moshfegh¹

AIVC 12056

¹Division of Energy and Production Systems
Department of Technology
University College of Gävle/Sandviken
S-801 76 Gävle, Sweden
²Department of Built Environment
Royal Institute of Technology
S-801 02 Gävle, Sweden

ABSTRACT

The thermal comfort of occupants is directly related to a number of parameters such as velocity of airflow, turbulence intensity and temperature distribution of room air. Thus the knowledge of the characteristics of the above-mentioned parameters is crucial for design engineers and knowledge of the turbulent properties is also important for improving the CFD codes. The present paper describes the experimental investigation of the flow field in a warm plane air jet under the influence of a heat sink in an insulated room. The purpose of this work is to establish how the turbulent fluctuations are distributed over different frequencies as a function of the Archimedes number. In addition to the local maximum velocity, the turbulence intensity and the turbulence length scale, the properties of velocity fluctuations in terms of autocorrelation function and the spectral density are investigated experimentally. The measurements are made at different distances from the supply for Reynolds numbers varying from 1514 to 8689 and for the corresponding Archimedes numbers between $2.69 \cdot 10^{-4}$ and $4.22 \cdot 10^{-6}$.

KEYWORDS

Full-scale experiment, Jet, Turbulent, Spectral analysis

INTRODUCTION

The thermal comfort of occupants is directly related to a number of parameters such as velocity of airflow, turbulence intensity and temperature distribution of room air. Thus the knowledge of the characteristics of the above-mentioned parameters is crucial for design engineers and knowledge of the turbulent properties is also important for improving the

Computational Fluid Dynamics (CFD) codes.

Turbulent fluctuations of velocity are important because the sensation of draught is assumed to be dependent on the magnitude of the velocity fluctuation. Furthermore there is a dearth of statistical data of the turbulence for the conditions valid for room air flows. The availability of data is important for improvement of CFD codes in order to predict room air flows. To the best of the authors' knowledge there are few results reported on the statistics of turbulence of non-isothermal flow at room air conditions, see Hassani and Stetz (1994) and Yamada et al (1994).

The paper reports the experimental results obtained for a warm plane air jet and includes some fundamental definitions of a turbulent flow field and spectral dynamics of turbulence. The flow conditions in a warm air wall jet are also summarised. The standard deviation and the properties of the velocity fluctuations in terms of their autocorrelation function and the spectral density are measured and the results of the measurements and numerical treatment are presented here. The experimental investigation is carried out for the warm plane air jet, spread horizontally from a slot under the ceiling in a well-insulated room where the floor is partly covered by a cooling panel. This paper reports the results from an ongoing research project on the characteristics of the warm and cold plane air jet, see Amiri et al (1996).

SOME FUNDAMENTAL RELATIONS

Some definitions will be given of the turbulent fluid variables, energy spectra and autocorrelation function. Thereafter, experimental arrangements for a warm plane air jet are presented. For stationary

turbulence the fluctuating variable, e.g., $u(t)$, at a specified location, x , can be presented by the composition of two parts, namely a time average and a fluctuating part and can be represented mathematically by

$$u(t) = U + u'(t) \quad (1)$$

where, U , the time average of, $u(t)$, during the integration time, τ , can be expressed by the Eulerian method as

$$U = \lim_{\tau \rightarrow \infty} \frac{1}{\tau} \int_0^\tau u(t) dt = \frac{1}{N} \sum_{i=1}^N u_i \quad (2)$$

The last equality in equation (2) derives, U , by means of the experimental (ensemble-averaging) results, where, N , is the total number of independently measured samples. By definition, the mean value of the fluctuating component, $u'(t)$, is zero, while the mean square value of the fluctuating component gives the variance of the fluctuating component, $\sigma_{u'}^2$;

$$\begin{aligned} \sigma_{u'}^2 &= \overline{u'^2} = \lim_{\tau \rightarrow 0} \frac{1}{\tau} \int_0^\tau (u')^2 dt = \\ &= \frac{1}{N-1} \sum_{i=1}^N (u_i - U)^2 \end{aligned} \quad (3)$$

The last equality in equation (3) derives the variance by the experimental results. The turbulence intensity can be introduced here by calculating the square root of equation (3). The ratio between the standard deviation, $\sigma_{u'}$, and the mean value of the fluctuating component, U , represents the relative turbulence intensity, I .

$$I = \frac{\sigma_{u'}}{U} \times 100 \quad (4)$$

The measurement of turbulence intensity is of great importance for the indoor climate because the sensation of draught depends on the magnitude of velocity fluctuation. The energy spectrum, $E_{u'}(f)$, of a fluctuating velocity component, $u'(t)$, presents the distribution of fluctuation energy, $\overline{u'^2}$, as a function of frequency, f . The distribution function, $E_{u'}(f)$, is called the power spectral density. The integral of the distribution function is equal to the variance, $\sigma_{u'}^2$, see Etheridge and Sandberg (1996):

$$\sigma_{u'}^2 = \overline{u'^2} = \int_0^\infty E_{u'}^+(f) df \quad (5)$$

The autocorrelation function of the fluctuating velocity component, $u'(t)$, at the same point is defined as

$$R_{u'}(\Delta t) = \lim_{\tau \rightarrow \infty} \frac{1}{\tau} \int_0^\tau u'(t) u'(t + \Delta t) dt \quad (6)$$

where, Δt , is the time lag. The normalised energy spectrum, $E_{u'}(f)/\overline{u'^2}$, and the autocorrelation function are coupled mathematically to each other by the following equation (they are a Fourier-transform pair) for positive frequencies

$$\frac{E_{u'}^+(f)}{\overline{u'^2}} = 4 \int_0^\infty e^{-i(\Delta t)f} R_{u'}(\Delta t) d(\Delta t) \quad (7)$$

Variation of the spectral energy as a function of frequency can be divided into three frequency ranges, namely energy containing, inertial and viscous dissipation. In the inertial range, the intermediate eddies make the main contribution to transfer or cascade, the kinetic energy in the turbulence to the smaller and finer scales of turbulent motion. The inertial range acts as a link between the two extremes of the turbulent spectrum. Analysis shows that in the inertial range the energy spectrum, $E_{u'}$, is proportional to the, $k^{-5/3}$, or so called Kolmogorov's law, see Hinze (1975).

$$E_{u'} = 1.5 \cdot \varepsilon^{2/3} \cdot k^{-5/3} \quad (8)$$

The turbulent length scale can formally be defined by

$$L_x = U \cdot L_t \quad (9)$$

where, L_t , is the integral time scale and this is the time the autocorrelation coefficient, $R_{u'}(\Delta t)/\overline{u'^2}$, takes to fall to e^{-1} . The integral time scale is obtained from the autocorrelation measurements. For the non-isothermal wall jets, the strength of the local Archimedes number is a vital parameter for distinguishing different flow characteristics, i.e. the jet still behaves like a jet or it is changed to a plume-like jet. By comparing

the magnitude of the initial momentum flux and the specific buoyancy, the transition from the jet-like to the plume-like behaviour can be defined. The distance where the transition occurs is called the thermal length, L_m . For non-isothermal cases the thermal length is used as the appropriate length scale for normalisation of the distance in this study. The thermal length, L_m , for non-isothermal plane jets is defined as (see Etheridge and Sandberg 1996):

$$L_m = b / (Ar_{in})^{2/3} \quad (10)$$

where, b , is the characteristic length of the inlet and, Ar_{in} , the supply Archimedes number represents the ratio of the buoyancy force to the inertia force at the supply point of the wall jet.

EXPERIMENTAL ARRANGEMENT

The employed wall-jet facility is shown in figure 1. It consists of a fan, a well-insulated room sized (LxWxH) 6x3x2.95 m as shown in figure 1. The air flow provided by a fan, passes through a heated element and is horizontally discharged through a slot with an aspect ratio (width to height) of 300:1 to form a two-dimensional wall jet. The height of the slot, b , is 0.01m. The air leaves the room through an opening in the same wall, see figure 1. A cooling panel is used as a heat sink which partly covers the floor to absorb the heat delivered to the room by the jet. The effect of the heat sink is estimated by measuring the mass flow rate of the

circulating media and its temperature at the inlet and outlet of the panel.

Seventy thermocouples are used in order to measure the wall surface temperature, room air and ambient temperature, and the inlet and outlet air temperature. Copper-constantan thermocouples are used for temperature measurements. All thermocouples are calibrated before the measurements. The maximum uncertainty for the temperature measurements is $\pm 0.3^\circ\text{C}$. Specially made traversing equipment is used for measuring the local air temperature and velocity at the same time. The local air velocity and temperature are recorded at different distances from the slot expressed in normalised form, $x/b = 12, 45, 70, 100, 150, 200, 300$ and 400 .

All measurements are conducted by using a Dantec anemometer 56C01-56C14 and a hot-wire of type 55R76. The output signal of the anemometer is digitised and a computerised evaluation procedure is employed. The hot-wire anemometer is calibrated before measurements. The Siddal and Davis (1972) calibration law is employed for the conversion of the anemometer voltage into velocity. Long integration times, of the order of 5 to 10 minutes, are utilised to obtain a good statistical accuracy. The sampling frequency is 400 Hz and the filtering frequency (low pass) is 40% of the sampling frequency. The spectral density, turbulence intensity and turbulent length scales are recorded at the point of maximum velocity.

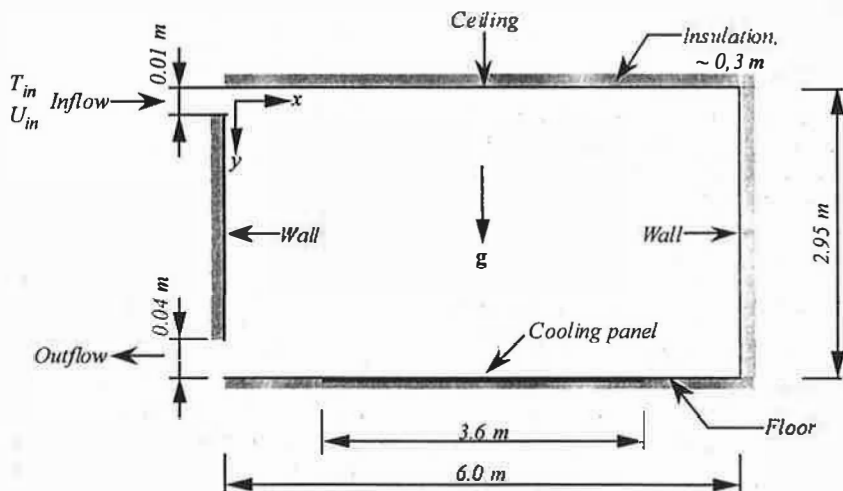


Figure 1 Geometry of the room under consideration.

RESULTS AND DISCUSSIONS

In this section, experimental results conducted with a warm plane air jet supplied to a well insulated room where the floor is partly covered by a cooling panel, are presented. A warm plane air jet can be described as a positively buoyant jet held to the ceiling by buoyancy forces. To compare the behaviour of the warm jet, five different cases have been studied. The first case is the reference case for this study, i.e. the isothermal case. Table 1 summarises the investigated cases.

Table 1 Summary of the experimental cases.

Case	U_{in} [m/s]	T_{in} [°C]	P_h [kW]	Re_{in} [-]	$Ar_{in} \cdot 10^{-5}$ [-]	L_m [m]
1	13.63	-	-	8689	0	∞
2	10.96	23.93	0.5	6988	4.22	38.29
3	6.98	28.03	2.0	4453	13.6	17.55
4	6.52	31.97	2.75	4156	21.1	13.10
5	2.37	34.00	2.0	1514	269	2.4

In Table 1, P_h stands for heating load. The ratio of the inertia force to the friction force at the supply point of the wall jet can be expressed by the Reynolds number, Re_{in} , and the ratio of the buoyancy force to the inertia force at the supply point of the wall jet can be expressed by the Archimedes number, Ar_{in} .

$$Re_{in} = \rho U_{in} b / \mu$$

$$Ar_{in} = g\beta(T_{in} - T_{ref})b/U_{in}^2$$

where ρ and μ are the density and dynamic viscosity of the air, calculated at a reference temperature of 27°C and T_{ref} is the room temperature, T_{in} the air supply temperature, U_{in} is the supply air velocity and β is the thermal expansion of the air.

The normalised local maximum velocity and the corresponding turbulence intensity profiles of the warm plane air jet

Figure 2 shows the normalised local maximum velocity, U_{max}/U_{in} , and the corresponding turbulence intensity, I , profiles at different downstream locations from the supply for the non-isothermal cases, see Table 1. For the non-isothermal cases, the proper length scale for normalisation of the distance is the thermal length, L_m , see equation (10).

As shown in figure 2, the decay rate of, U_{max}/U_{in} , for case 2 to 5, has a power law relationship with normalised downstream location from the supply, x/L_m . The slope of the lines in log-log scales varies between -0.54 and -0.51, showing a great similarity between the cases. Based on the theory for two-dimensional jet, the slope of decay rate of, U_{max}/U_{in} , in log-log scales is -0.5. The same behaviour is also observed for the growth of the turbulence

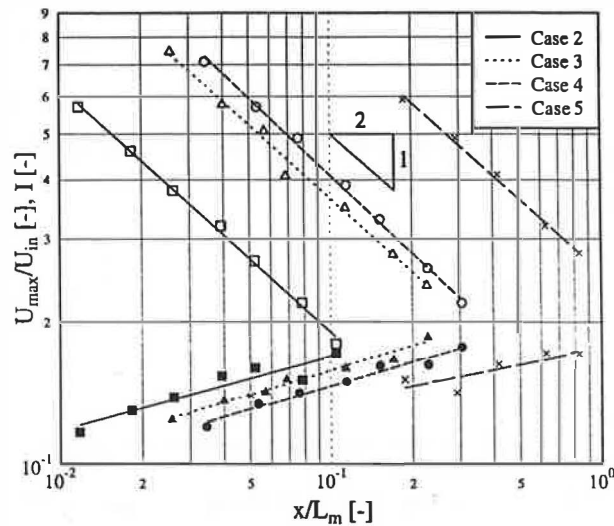


Figure 2 The measured normalised local maximum velocity, U_{max}/U_{in} , and turbulence intensity, I , profiles at different downstream locations from the supply.

Table 2 Measurement results of the turbulence intensity at different downstream locations from the supply for all cases.

x/b [-]	I (case 1) [%]	I (case 2) [%]	I (case 3) [%]	I (case 4) [%]	I (case 5) [%]
12	8.26	6.52	28.01	9.83	13.92
45	13.03	11.69	12.42	12.00	15.08
70	13.71	13.01	13.64	13.36	14.17
100	14.45	13.86	14.29	14.17	16.32
150	14.94	15.37	15.20	14.96	17.18
200	15.39	16.02	16.05	16.14	17.03
300	15.50	15.08	16.72	16.23	21.06
400	16.35	17.11	18.70	17.72	25.33

intensities at the local maximum velocity points except for case five where the changes are slower. The variation of the turbulence intensity at different downstream locations from the supply for all cases is summarised in Table 2

It is worth pointing out that the turbulence intensity has a tendency to increase with increasing Archimedes numbers. For all cases the turbulence intensity at the beginning increases by an increasing distance from the supply for finally becoming almost (self similar) for, x/b , between 100 and 200.

The growth of the turbulent length scale

The measured normalised turbulence length scale (integral scale), L_s/L_m , as a

function of the normalised downstream locations, x/L_m , is shown in figure 3. The growth of the turbulent length scale is almost linear for the presented cases. For case 2, 3 and 4 the slope of the line is in good agreement with the result obtained by Sandberg et al (1991) and Karimipannah and Sandberg (1996), or in other words, they behave nearly like two-dimensional isothermal wall jets. For case five the rate of growth of the turbulent length scale is much slower than for the other cases. This can be interpreted as being an effect of the buoyancy force. The values of the length scale are important for the grid structure in the numerical analysis. As shown in figure 3, a finer grid must be applied close to the inlet region and also the near-wall region

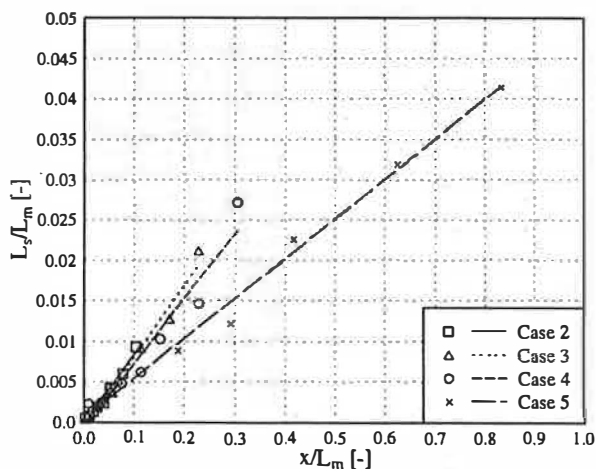


Figure 3 The growth of the turbulent length scale for the non-isothermal cases.

The normalised power spectral density and the corresponding autocorrelation function

Figure 4 shows the recorded normalised power spectral density and the corresponding correlation function at $x = 1.50$ m from the supply for all cases. As it is shown in figure 4(a), the slope of the energy spectrum in the inertial range is in good agreement with the Kolmogorov's law, $k^{-5/3}$, see equation (8).

At very low frequencies, less than 10 Hz, some differences can be observed for the energy spectrum. For case five, with the highest buoyancy force, the frequency band of inertial range is smaller compared to

other cases. One possible explanation is that the supply Reynolds number is rather low for case five. Based on the theory, for isothermal conditions of the spectral density, the band of the inertial range increases with increasing Reynolds number. It is also notable that when the Ar_{in} becomes as high as $2.69 \cdot 10^{-4}$ there is a noticeable effect of the buoyancy on the turbulent properties of the jet and for Ar_{in} less than 10^{-5} , the jet properties are very similar to isothermal jets. Figure 5 shows the recorded normalised power spectral density at different downstream locations for case one and five.

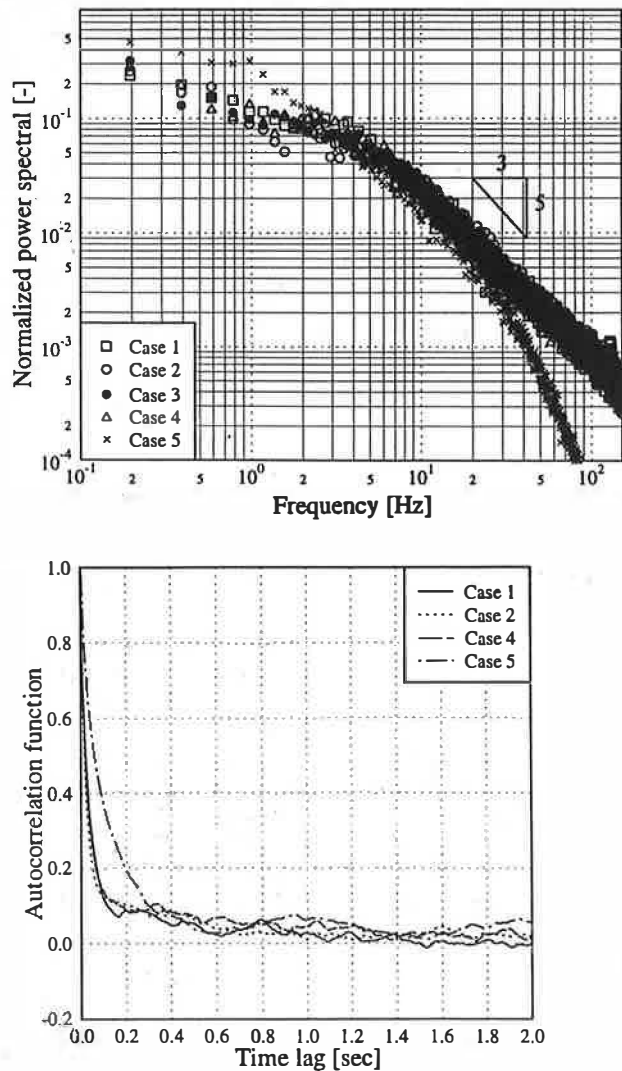


Figure 4 The recorded normalised power spectral density and the corresponding autocorrelation at $x = 1.50$ m for all cases.

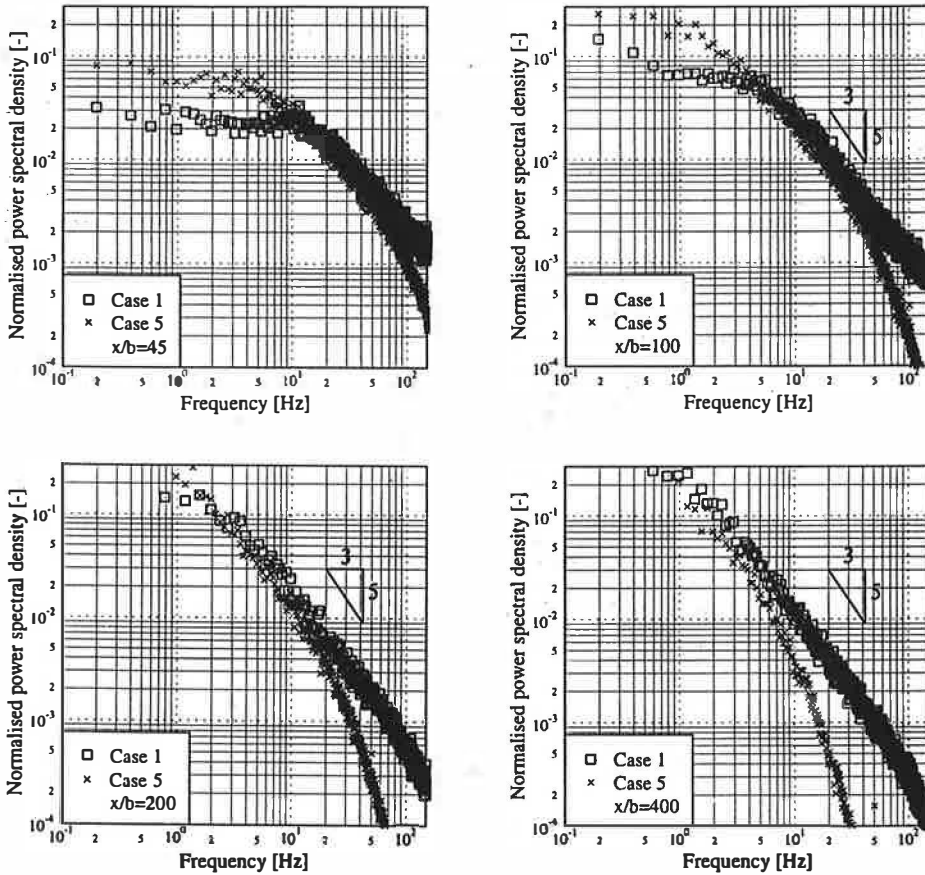


Figure 5 The recorded normalised power spectral density at different downstream locations for case one and five.

CONCLUSIONS

The present experiment reveals that the decay rate of, U_{max}/U_{in} , has for all cases a power law relationship with a decay rate between -0.54 and -0.51. For all cases the turbulence intensity at the beginning increases by an increasing distance from the supply for finally becoming almost constant (self similar) for, x/b , between 100 and 200. The turbulent length scale (integral scale) grows linearly in the downstream direction. However, for the case with the highest Archimedes number, $Ar_{in} = 2.69 \cdot 10^{-4}$, the growth is much smaller than for the other cases. The measured turbulent length scale is of importance for the grid refinement in the numerical analysis. The recorded normalised power spectral density shows good agreement with the Kolmogorov's law,

$k^{-5/3}$, in the inertial range. However, again for the case with the highest buoyancy force, the frequency band of inertial range is smaller than in other cases. In summary, when the supply Archimedes number becomes as high as $2.69 \cdot 10^{-4}$ there is a noticeable effect of the buoyancy on the turbulent properties of the jet. When the Archimedes number is less than 10^{-5} the jet properties are very similar to isothermal jets.

ACKNOWLEDGEMENTS

The authors wish to thank Mr Claes Blomqvist at the Department of Built Environment, Royal Institute of Technology, Gävle, Sweden for his help during this work. Support of this work by the University College of Gävle/Sandviken, Gävle, Sweden is gratefully acknowledged.

REFERENCES

Amiri, S., Sandberg, M. and Moshfegh, B. (1996). Effect of Cooling Loads on Warm Plane Air Jet. *Proceedings ROOMVENT '96*. Yokohama, Japan.

Etheridge D. and Sandberg M. (1996). *Building Ventilation Theory and Measurements*. John Wiley & Sons. Chichester. UK.

Hassani, V. D. and Stetz, M. (1994). Effect of Local Loads on Separation of Negatively Buoyant Wall Jets in Enclosed Spaces, *Proceedings of ROOMVENT '94*. Krakow, Poland.

Hinze, J. O. (1975). *Turbulence*. McGraw-Hill, Inc. New York.

Karimipannah, T. and Sandberg, M. (1994). Deflection and Influence of Room size of a Two-dimensional Wall Jet in a Ventilated Room. *Proceedings of ROOMVENT '94*. Krakow, Poland.

Karimipannah, T. (1996). Behaviour of Jets in Ventilated Enclosures. *Proceedings of ROOMVENT '96*. Yokohama, Japan.

Sandberg M., Blomqvist, C. and Mattsson, M. (1991). Turbulence Characteristics in Rooms Ventilated with a High Velocity Jet, *Proceedings 12th AIVC Conference*. Ottawa, Canada.

Yamada, N., Kubota, H., Kurosawa, K., Yoshida Y. and Hanaoka, Y. (1994). Local Space Heating by Covering with Warm Plane Jet. *Proceedings of ROOMVENT '94*. Krakow, Poland.